Surface catalytic effect on chemical heat flux using direct simulation Monte Carlo

Youngil Ko[1], Eunji Jun[1]

Abstract

Designing a Thermal Protection System (TPS) for re-entry vehicles requires numerical methods due to the difficulties in experimentally replicating the highly non-equilibrium flows. The Direct Simulation Monte Carlo (DSMC) method stands out for its effectiveness in capturing the non-equilibrium characteristics. This study assesses the effects of different molecular models and relaxation schemes within DSMC on the simulation of rarefied hypersonic flow around a 2D cylinder. Results show that the choice of molecular model and gas-phase relaxation scheme affects the surface heat flux and flowfield temperature prediction, respectively. Furthermore, a parametric analysis of the surface catalytic recombination in DSMC is conducted by adjusting the surface recombination coefficient, γ. The noncatalytic surface ($\gamma = 0$) and fully-catalytic surface ($\gamma = 1$) serve as the upper and lower bounds of the predicted total heat flux. Additionally, the chemical heat flux at the stagnation point increases with the surface recombination coefficient, due to the exothermicity of the recombination reaction, while translation heat flux remains nearly unaffected by surface catalysis.

Keywords: *DSMC, Rarefied Gas Dynamics, Gas-surface Interactions, Surface Catalysis*

Nomenclature

Latin
b − aspe line of collision
c − molecule speed
d − molecule diameter
n − number density
q − heat flux
T − temperature
V − velocity
x − distance along the stagnation line
y − distance along the height of the cylinder
from the centre of 2D cylinder

Greek

α − VSS deflection parameter
γ − surface recombination coefficient
χ − deflection angle
ω − viscosity-temperature index

Subscripts
r − the relative value of two colliding particles
ref − reference value
rot − rotational
w − wall/surface
∞ − freestream
tr − translational
vib − vibrational

1. Introduction

The introduction of SpaceX reusable launch system technology has reduced the costs associated with space launches. Central to this achievement is the Thermal Protection System (TPS), which is crucial for protecting the spacecraft from the intense heat generated by atmospheric friction during re-entry. Notably, the mass of the TPS can account for up to half of the vehicle's total weight, highlighting the importance of designing it to be efficient [1]. Designing TPS for extreme conditions presents many challenges due to the difficulties in experimentally replicating the high-enthalpy flow conditions experienced during actual flight. Re-entry flows are characterized by extreme temperatures, resulting in complex real-gas effects such as thermal relaxation and dissociation reactions of air molecules. Given

---

these experimental constraints, numerical modeling methods play a crucial role in the development of TPS.

The aerodynamic flow around re-entry vehicles is highly non-equilibrium, due to the rarefied atmospheric conditions and the formation of a strong shock wave. The Navier-Stokes equation falls short of capturing the non-equilibrium phenomena because of its inherent continuum assumption. In contrast, the Boltzmann equation, which does not rely on the continuum assumption, can be a more accurate governing equation for re-entry flows. In particular, the Direct Simulation Monte Carlo (DSMC) method is a widely adapted numerical method for resolving the Boltzmann equation [2]. However, implementing DSMC for TPS in re-entry vehicles introduces distinct challenges, particularly in ensuring that the models accurately reflect the real-gas effects. For example, the choice of molecular model affects the behavior of simulation particles during gas-phase collisions. Changing the gas-phase relaxation scheme can alter the rate of internal energy relaxation and can change the local flowfield temperature. Additionally, the surface catalytic conditions play a crucial role in determining the heat flux on the vehicle surface. Therefore, it is imperative to critically evaluate the sensitivity of DSMC results to variations in employed models.

This study aims to assess the impact of different models and schemes within the DSMC method on the simulation of rarefied hypersonic flow. It involves an evaluation of various molecular models and relaxation schemes for internal energies, which are used to represent the dynamics of gas particles during gas-phase collisions. Furthermore, the study conducts a parametric analysis of the surface recombination coefficient of atoms upon collision with surfaces. The study uses a benchmark rarefied hypersonic flow of air over a 2D cylinder for all simulations for comparison.

2. Numerical Methodology and Physical Model

2.1. Direct Simulation Monte Carlo

The simulation of rarefied hypersonic flows requires a kinetic approach, making the Boltzmann equation a suitable governing equation due to its ability to accurately capture the gas kinetics across different flow regimes. The DSMC method numerically solves the Boltzmann equation by tracking the motion and collisions of simulation particles, and by stochastically calculating their macroscopic properties in each grid [2]. The schematic of the DSMC method is outlined in Fig.1A, starting with the selection of a molecular model for the simulation particles. Simulation particles are moved and tested for gas-phase or gas-surface collision, triggering the corresponding collision mechanism as needed.

This study utilizes the Stochastic PArallel Rarefied-gas Time-accurate Analyzer (SPARTA), a DSMC code developed by Sandia National Laboratories [3]. This open-source code is known to support accurate simulation of hypersonic gas dynamics in rarefied conditions.

2.2. Gas-phase: Molecular Model

The DSMC method utilizes simulation particles to replicate the behavior of real gas molecules. As illustrated in Fig.1B, the binary collision process at the microscopic scale involves parameters such as molecular diameter, d, length of the aspe line, b, and relative speed of the colliding particles, c_r. An effective molecular model for DSMC should convert these microscopic collision parameters into observable real-gas effects, such as temperature-dependent viscosity represented as a power of ω at the macroscopic scale [1]. The Hard Sphere (HS) model is one of the simplest molecular models. The diameter, d, remains constant irrespective of c_r of two colliding particles. The deflection angle, χ, is solely determined by d and b, resulting in isotropic collisions. Despite its simplicity, the HS model lacks accuracy in describing the scattering behavior and predicting the temperature dependence of the viscosity of real gases.

To address these shortcomings, Bird introduced the Variable Hard Sphere (VHS) model, which allows d to vary with c_r as a function of the temperature-viscosity index, ω [4]. The adaptation better reflects the temperature-dependent viscosity. Yet, the VHS model still falls short in predicting a correct Schmidt number, Sc, which represents the ratio of viscosity to diffusion for the gas modelled. In response, Koura and Matsumoto developed the Variable Soft Sphere (VSS) model, introducing the VSS deflection parameter, α, to adjust the collision anisotropy and phenomenologically replicate the mass diffusivity of real gas [5].

Table 1 shows a list of equations describing the diameter and deflection angle of two colliding particles across different molecular models. The list highlights the increasing complexity of the molecular model. The parameters of each model are derived through the first-order approximation of the Chapman-Enskog theory, providing kinetic-based closed-form solution for transport properties [6]. Thus, the coefficients associated with the VHS and VSS models can be interpreted as a phenomenological representation of real gases.
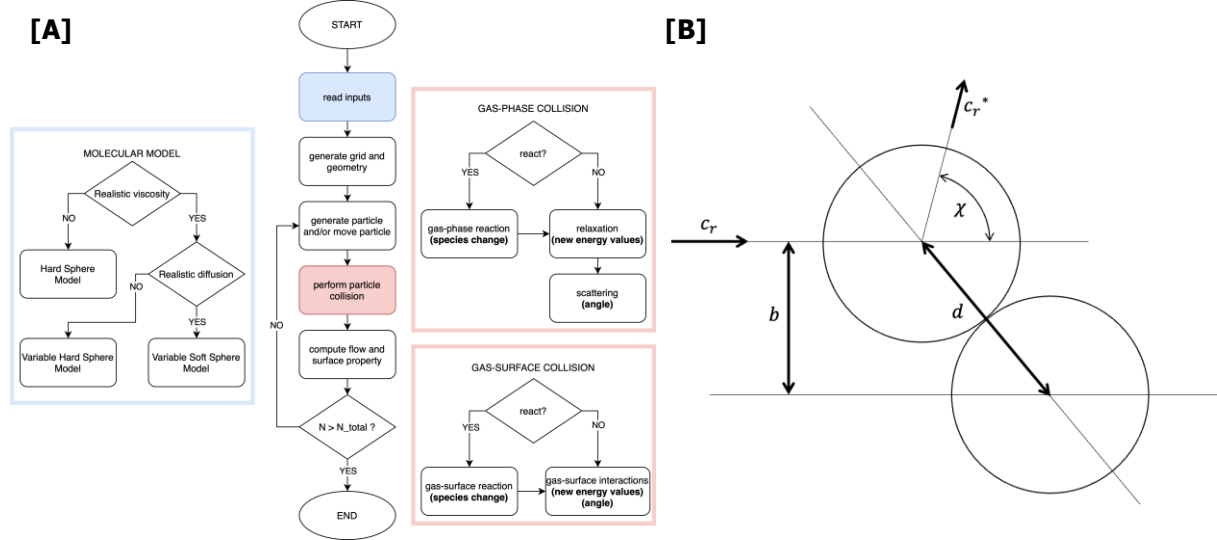
[A]   **[B]**

Fig 1. [A] Flowchart of the DSMC method. [B] Gas-phase collision parameters.

Table 1. Equations for three phenomenological molecular models for simulation particles.

Molecular Model	Diameter (m)	Deflection Angle (°)	Parameters
Hard Sphere (HS)	$d = d_{ref}$	$\chi = 2\cos^{-1}\{(b/d)\}$	d_{ref}
Variable Hard Sphere (VHS)	$d = d_{ref}\left(c_{r.ref}/c_r\right)^{\omega-0.5}$	$\chi = 2\cos^{-1}\{(b/d)\}$	$d_{ref},\ c_{r.ref},\ \omega$
Variable Soft Sphere (VSS)	$d = d_{ref}\left(c_{r.ref}/c_r\right)^{\omega-0.5}$	$\chi = 2\cos^{-1}\{(b/d)^{1/\alpha}\}$	$d_{ref},\ c_{r.ref},\ \omega,\ \alpha$

2.3. Gas-phase: Relaxation Scheme

When two gas particles collide, their translational, rotational, and vibrational energies are redistributed toward achieving thermal equilibrium. The rate of energy relaxation is especially critical in hypersonic flow, where the flow's characteristic time may be comparable to the relaxation rate [7,8]. A slower relaxation rate implies that more thermally non-equilibrium gas beyond the shock may interact with the surface. At the macroscopic scale, the Landau-Teller (LT) equation characterizes the relaxation rate of internal energy modes towards equilibrium [9]. In DSMC, the Larsen-Borgnakke (LB) model is employed to replicate the relaxation rate predicted by the LT equation [10]. DSMC requires a mechanism to select collision pairs and determine if they undergo energy relaxation as per the LB model. Two popular gas-phase relaxation schemes for contemporary DSMC solvers are: a) "permitting double-relaxation" [2], and b) "prohibiting double-relaxation" [11,12].

Figs. 2A and 2B illustrate the simplified flowchart for the two schemes. In the "permitting double-relaxation" scheme, a collision pair is selected, and one of the particles undergoes testing for potential relaxation, followed by the other. Consequently, if both particles are selected for an inelastic collision, the relaxation sequence involves a certain degree of interdependence between their relaxation rates. Conversely, the "prohibiting double-relaxation" scheme relaxes only one of the particles of the collision pair, thereby eliminating the possibility of double relaxation. Although the current SPARTA code employs the "permitting double-relaxation" scheme, previous studies have shown its shortcomings in representing the LT equation near thermal equilibrium, and thus advocate for the "prohibiting double-relaxation" method [12].
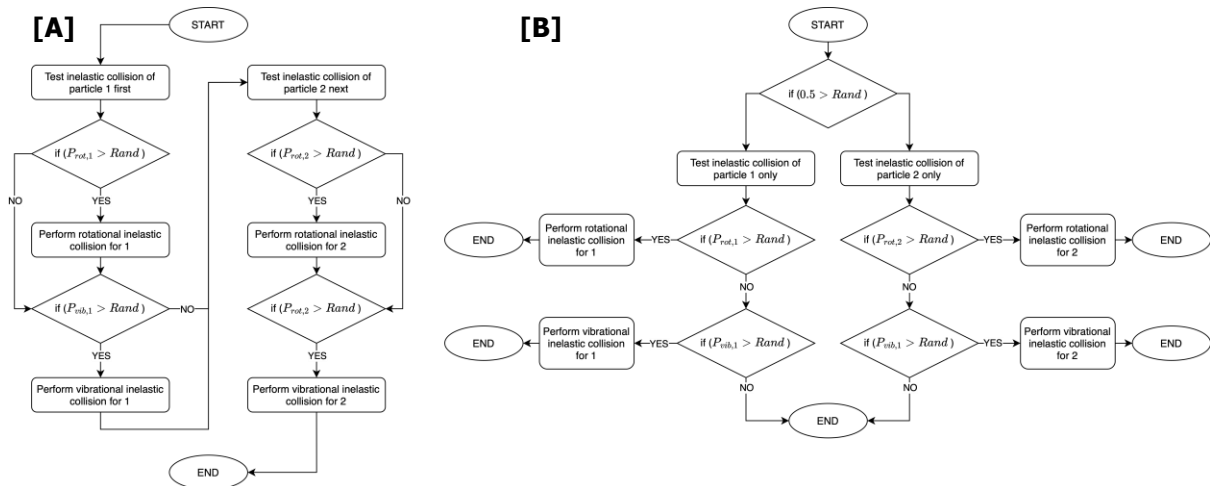
Fig 2. [A] "Permitting double-relaxation" scheme. [B] "Prohibiting double-relaxation" scheme

2.4. Gas-surface: Interaction and Surface Reaction

Gas-surface interactions (GSI) are critical in determining surface properties such as heat transfer, and pressure when gas molecules collide with solid surfaces. Accurate GSI modeling requires capturing the complex physical and chemical processes involved. In DSMC, GSI is modelled by defining the post-collision behavior of gas particles, including their velocity, internal energy, and scattering angle. Common models used in DSMC for GSI are Maxwell and CLL, which account for thermal accommodation (or thermalization) to the isothermal surface temperature, as shown in Fig. 3A [13].

Additionally, GSIs can involve surface reactions, notably heterogeneous catalytic recombination reactions, where surface catalysis leads to atom recombination into molecules. Due to its exothermicity, the reactions can significantly increase heat flux to the surface. The degree of heterogenous recombination can vary by surface material and the relative reaction rates. The surface recombination coefficient, γ, can be used to measure the degree of surface recombination, as γ quantifies the fraction of atoms recombing on the surface, as shown in Fig. 3B.

Modeling surface catalytic reactions typically involves two extreme conditions: noncatalytic (NC) surface condition, assuming no heterogenous recombination (i.e., $\gamma = 0$), and fully catalytic (FC) surface condition, assuming complete recombination (i.e., $\gamma = 1$). Naturally, NC and FC conditions predict the minimum and maximum heat flux to the surface, respectively, which may differ by a factor of 3 [14]. Therefore, inaccurate predictions of heat flux can hinder the efficient design of the TPS. Typically, γ is inferred from experiments and used as an input for surface boundary conditions of numerical methods. However, it should be noted that the value of γ is a resultant global value that only provides the net effect of the complicated physicochemical phenomenon near the gas-surface interface. Hence, another approach such as modeling the finite-rate chemistry at the surface should be used and explored in future studies [14].
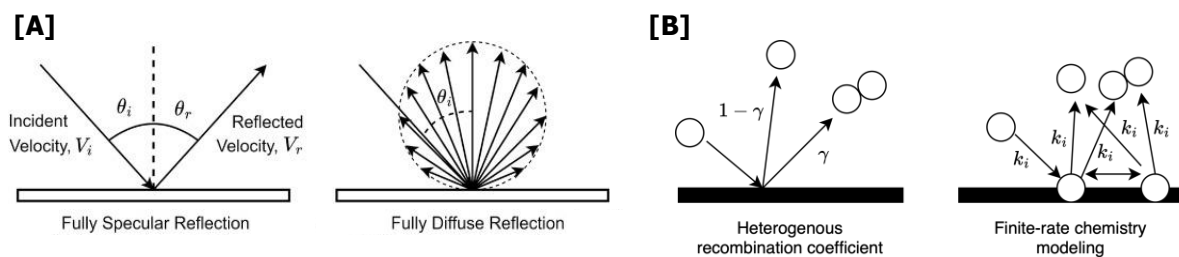

Fig 3. [A] Maxwell Gas-surface interactions. [B] Surface Chemistry modeling techniques.

3. Results and Discussion

3.1. DSMC Setup

To assess the impact of various models and parameters within the DSMC method, a benchmark test case of rarefied hypersonic flow around a 2D cylinder is used [15]. The specific input conditions for the simulations are presented in Table 2. Since macroscopic properties are statistically sampled from the simulation particles within each grid cell, a sufficient number of simulation particles per grid cell is required. Therefore, adaptive mesh refinement is employed in all simulations to ensure a minimum of 20 simulation particles per cell. Moreover, the grid size near the surface is restricted to less than one-tenth of the local mean free path for accurate calculation of surface properties. The timestep is set to 5E-8 seconds, shorter than the minimum local mean collision time to maintain accurate temporal resolution.

Table 2.   Input conditions for the benchmark DSMC hypersonic test case [13].

d_w (m)	V_∞(m/s)	T_∞ (K)	T_w (K)	$n_{N_2,\infty}$ (1/m^3)	$n_{O_2,\infty}$ (1/m^3)
2	6813	187	1000	1.13E20	3.031E19

The results are categorized as nonreacting or reacting, depending on whether gas-phase chemical reactions are included. All "reacting" simulation use the TCE chemistry module, with 11 chemical reactions that include dissociation and exchange reactions among five air species (O_2, N_2, O, N, NO). Reaction coefficients are based on Arrhenius rates of reactions rates [16]. Consistent with the benchmark case from [15], rotational and vibrational collision numbers are set at 5 and 50, respectively.

3.2. Effect of Molecular Model and Parameter

The molecular model and parameters used in the comparative study are summarized in Table 3. Bird VHS and Bird VSS, widely used in the DSMC community, are based on the data for the transport properties that were tabulated in Chapman and Cowling [2,17]. Note that the reference case used Bird VHS parameters.

Table 3.   Parameters used for the two molecular models used at $T_{ref} = 273$K [2]

Molecular Model		O_2	N_2	O	N	NO
Bird VHS	d_{ref} ($\times 10^{-10}$m)	4.07	4.17	3.00	3.00	4.20
	ω	0.77	0.74	0.80	0.80	0.79
Bird VSS	d_{ref} ($\times 10^{-10}$m)	4.01	4.11	3.00	3.00	4.00
	ω	0.77	0.74	0.80	0.80	0.80
	α	1.40	1.36	1.00	1.00	1.00

Fig. 4 illustrates the effect of different molecular models and parameters. Fig. 4A and Fig. 4B present the translational, rotational, and vibrational temperatures (T_{tr}, T_{rot}, T_{vib}) of gas molecules along the stagnation line for nonreacting and reacting flows, with benchmark results from Scanlon et al. [15]. In reacting flow, the peak T_{tr} is lower than that of the nonreacting flow due to the endothermic dissociation reactions. Both T_{rot} and T_{vib} respond more slowly to the to the sharp increase in T_{tr}, a consequence of the thermal relaxation process. The slower response of the T_{vib} is due to the higher vibrational collision number. An isothermal boundary condition normalizes all temperatures to 1000 K at the surface. The results suggest that variations in the molecular model have minimal impact on the flowfield temperature calculations.

Figs. 4C and Fig. 4D show the heat flux distribution along the noncatalytic surface of a 2D cylinder for nonreacting and reacting flows. The heat flux peaks at the stagnation point and decreases progressively along the cylinder's surface. The choice of molecular model significantly affects the heat flux calculation due to its sensitivity to the transport properties. In the hypersonic boundary layer, where viscous real-gas effects are significant, selecting a different molecular model can lead to variations in calculated

heat flux [18]. The difference is more pronounced in the nonreacting case (Fig. 4C) due to higher temperatures, compared to the reacting case (Fig. 4D) where endothermic reactions occur. Although simulations using the Bird VHS model show the closest agreement because benchmark references that also use Bird VHS values, it is crucial to acknowledge that this alignment does not necessarily validate the simulation results as a precise reflection of the physical phenomena under actual flight conditions.
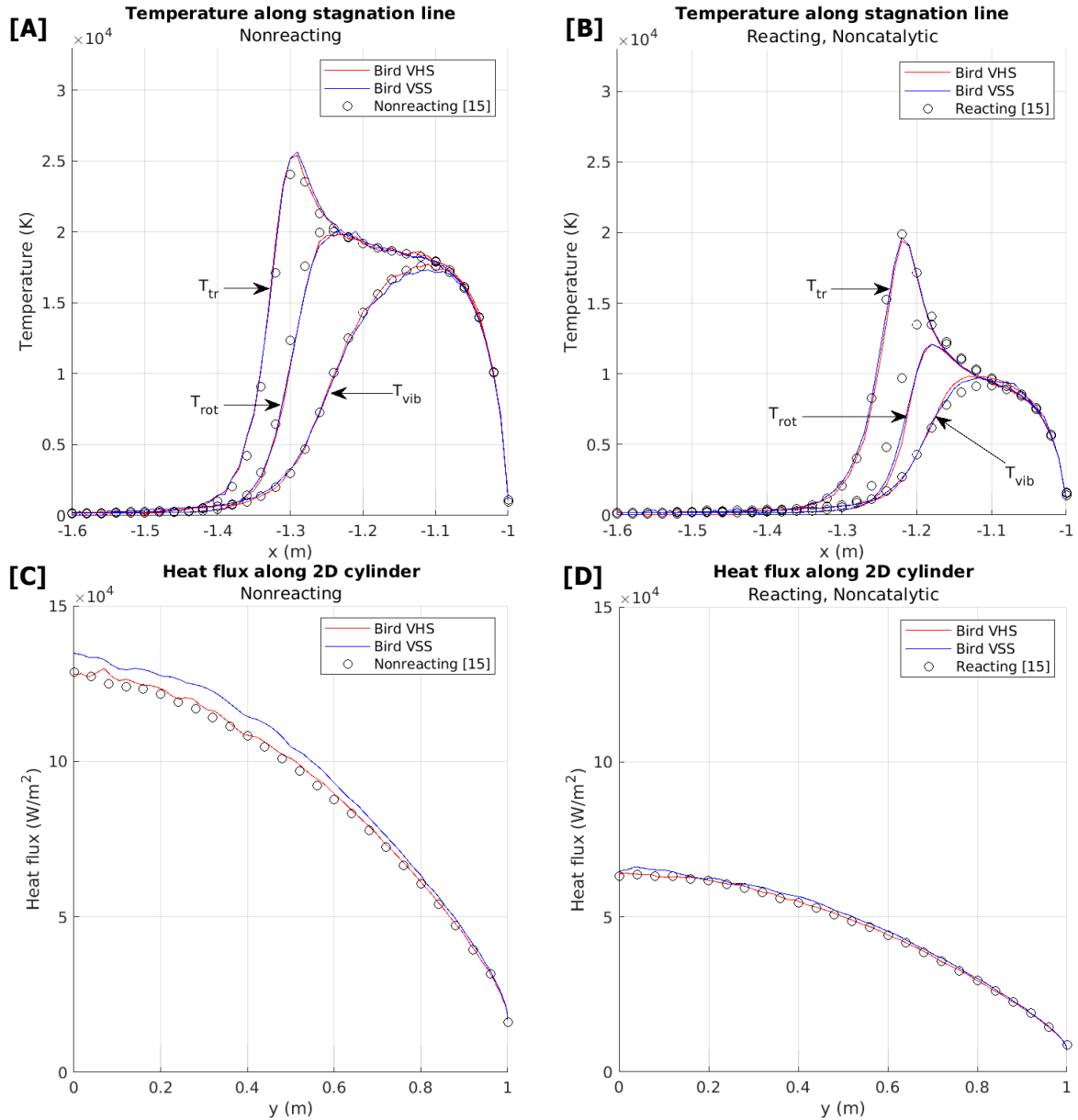

Fig 4. The effect of different molecular model on temperature along the stagnation line for [A] nonreacting case and [B] reacting case; and on heat flux along 2D cylinder for [C] nonreacting case and [D] reacting case.

3.3. Effect of Gas-phase Relaxation Scheme

The benchmark test case is used to compare two gas-phase relaxation schemes: "permitting double-relaxation" and "prohibiting double-relaxation" scheme. The comparative impact of these two gas-phase relaxation schemes is illustrated in Fig. 5, where Fig. 5A and Fig. 5B are the T_{tr}, T_{rot}, and T_{vib} of gas molecules along the stagnation line for nonreacting and reacting flows, respectively. The results demonstrate that the "prohibiting double-relaxation" scheme leads to faster relaxation of T_{rot} and T_{vib} towards thermal equilibrium, aligning consistent with results from prior studies [12]. The difference between the schemes is more significant in nonreacting flows with higher peak T_{tr} and higher local

thermal nonequilibrium within the shock structure. This leads to the wider gap between T_{tr} and T_{rot}, T_{vib} and hence a more significant difference in the relaxation rates predicted by the two schemes [19].

Figs. 5C and Fig. 5D depict the distribution of heat flux across the surface of the 2D cylinder. The surface heat flux predictions from both relaxation schemes agree well due to the isothermal surface boundary conditions implemented in both DSMC simulations. The high density and the increased gas-phase collision frequency after shock make a near-thermal equilibrium in the boundary layer near the stagnation point. Consequently, the two relaxation schemes show negligible differences in the heat flux predictions.
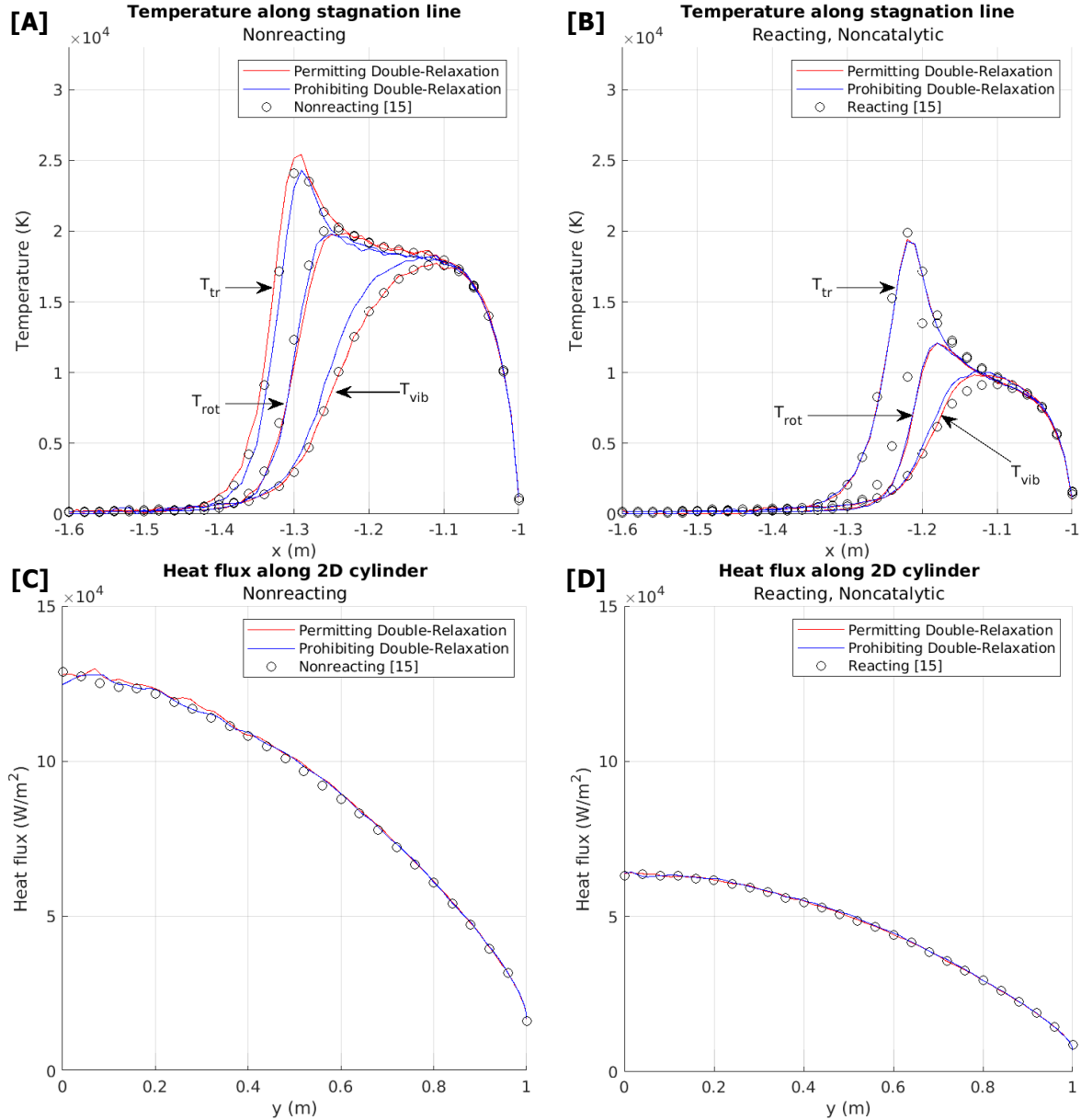

Fig 5. The effect of different relaxation scheme on temperature along the stagnation line for [A] nonreacting case and [B] reacting case; and on heat flux along 2D cylinder for [C] nonreacting case and [D] reacting case.

3.4. Effect of Surface Catalytic Recombination

In the SPARTA DSMC simulations, surface catalytic recombination is applied as a boundary condition. This study assumes equal surface recombination coefficient for oxygen and nitrogen (i.e $\gamma_{O_2} = \gamma_{N_2}$). To simulate heterogenous recombination, half of the recombining atoms form their diatomic molecules, while the other half are removed from the surface. Table 4 outlines the parametric values utilized to investigate the influence of γ.

Table 4. Modeling surface recombination coefficient in SPARTA DSMC

	Reaction	Probability	Recombination energy per particle ($\times 10^{-19}$J)
O_2 Recombination $\gamma_{O2} = \gamma$	$O \rightarrow NULL$	$\gamma/2$	0
	$O \rightarrow O_2$	$\gamma/2$	8.197
N_2 Recombination $\gamma_{N2} = \gamma$	$N \rightarrow NULL$	$\gamma/2$	0
	$N \rightarrow N_2$	$\gamma/2$	1.561

Table 5. Parameters for surface catalytic recombination.

Surface catalytic recombination				
Noncatalytic (NC)	Partially-catalytic (PC)			Fully-catalytic (FC)
0.0	[0,001, … ,0.009]	[0.01, … ,0.09]	[0.1, … ,0.9]	1.0

Fig. 6 illustrates the impact of surface catalytic conditions on gas dynamics. Fig. 6A is the O_2 number density contour around a 2D cylinder, demonstrating the effect of surface conditions. For fully-catalytic surface, all atomic oxygen colliding with the surface undergoes recombination, significantly increasing the local O_2 number density around the surface. Fig. 6B shows the number density of involved species along the stagnation line, noting that in both scenarios, the reacting flowfield causes a decrease in molecule number density due to gas-phase dissociation. Yet, from the shock's end to the boundary layer near the stagnation point, fully-catalytic conditions (dashed line), increase the concentration of recombined molecules compared to noncatalytic conditions, represented by (solid line).

Fig. 6C presents the heat flux distribution around a 2D cylinder under noncatalytic and fully-catalytic surface conditions, with a blue line indicating the heat flux in a nonreacting flowfield. The heat flux pattern in the fully-catalytic case resembles that of the nonreacting case, indicating that heat flux predictions are primarily influenced by the properties of the gas impinging on the surface, rather than the recombination location of atoms. This observation aligns with prior numerical studies, which concluded that the type of recombination (gas phase or on the surface) does not alter the heat flux under specified freestream conditions [20]. Fig. 6D shows the effect of the surface recombination coefficient, γ, affects heat flux contributions. The lowest and highest heat flux predictions correspond to noncatalytic and fully-catalytic conditions, respectively. The formation of diatoms from heterogenous recombination increases q_{rot} and q_{vib}. q_{chem} increases logarithmically with increasing γ. Interestingly, q_{tr} is almost constant with γ. This is largely due to the isothermal surface condition and the high density near the stagnation point where T_{tr} remains close to T_w. The summation of the heat flux components leads to a characteristic S-shaped increase in total heat flux with γ for partially-catalytic surfaces.

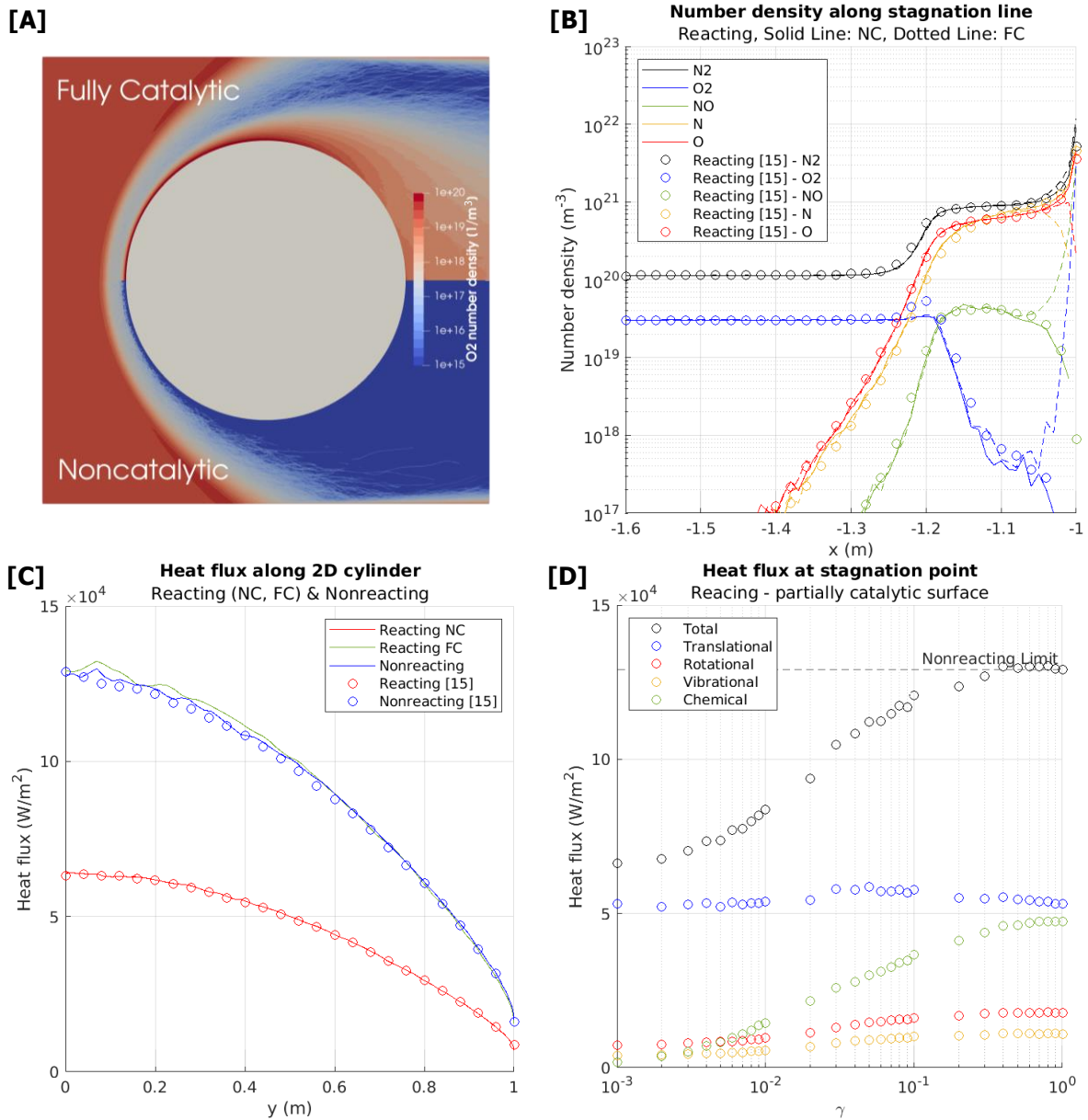**[A]**

[B]

[C]

[D]

Fig 6. The effect of surface catalytic condition on [A] flowfield; [B] number density along the stagnation line; [C] heat flux along 2D cylinder; and [D] peak stagnation heat flux.

4. Conclusion

This study assesses the impact of various models and schemes employed in the DSMC method, particularly in the context of rarefied hypersonic airflow around a 2D cylinder, which serves as a benchmark for comparative analysis. The study reveals that the choice of molecular model significantly influences heat flux predictions on the cylinder's surface, attributed to differences in collision mechanics when gas atoms interact with the surface. Furthermore, the two examined gas-phase relaxation schemes exhibit discrepancies in temperature relaxation rates across the shock layer, especially noticeable as the peak translational temperature rises in nonreacting scenarios due to a pronounced local divergence between translational and rotational/vibrational temperatures.

Parametric analyses of the surface recombination coefficient, γ, indicate substantial variations in flowfield species distribution and heat flux predictions. Specifically, noncatalytic and fully-catalytic wall conditions yield the lowest and highest heat flux predictions at a given freestream condition, respectively. Analyses of partially-catalytic surfaces, modelled by assigning a constant γ value ranging between 0 and 1, demonstrate a significant dependence of stagnation point heat flux on increasing γ

values. While chemical, rotational, and vibrational heat fluxes escalate with γ, the translational heat flux remains relatively unchanged.

The findings in the study can be used as a reference for selecting appropriate gas-phase models in future rarefied hypersonic problems of blunt bodies using the DSMC method. However, the assumption of a catalytic wall characterized by a constant γ overlooks the complex surface catalytic phenomena, suggesting that a high-fidelity solution can be attained by the finite-rate chemistry effect at the gas-surface interface. Moreover, consideration of the chemical energy accommodation can provide a new parameterization of quantifying the contribution of the chemical energy caused by the exothermic surface recombination to the surface heat flux. Future research will delve into these aspects of gas-surface interactions, aiming to enhance the fidelity of the particle-based DSMC method.

Acknowledgments

References

1. Le, V.T., San Ha, N., Goo, N.S.: Advanced sandwich structures for thermal protection systems in hypersonic vehicles: A review. Comos. B. Eng. 226, 109301 (2021)

2. Bird, G.A.: A molecular gas dynamics and the direct simulation of gas flows, Oxford (1994)

3. Gallis, M.A., Torczynski, J.R., Plimpton, S.J., Rader, D.J., Koehler, T.: Direct simulation Monte Carlo: The quest for speed. AIP Conf. 1628, 27-36 (2014)

4. Bird, G.A.: Monte-Carlo simulation in an engineering context. Prog. Astronaut. Aeronaut. 74, 239-255 (1981)

5. Koura, K, Matsumoto, H.: Variable soft sphere molecular model for inverse-power-law or Lennard-Jones potential. Phys. Fluids A: Fluid Dynamics 3, 2459-2465 (1991)

6. Bird, G.A.: The DSMC Method, CreateSpace Independent Publish Platform (2013)

7. Jun, E., Boyd, I.D.: Assessment of the LD-DSMC hybrid method for hypersonic rarefied flow. Comput. Fluids 166, 123-138 (2018)

8. Jun, E., Burt, J.M., Boyd, I.D.: All-Particle Multiscale Computation of Hypersonic Rarefied Flow. In AIP Conf. Proc. 1333(1), 557-562 (2011)

9. Landau, L. Teller, E.: On the theory of sound dispersion, Physik. Z. Sow. 10 34-43 (1936)

10. Borgnakke, C, Larsen, P.S.: Statistical collision model for Monte Carlo simulation of polyatomic gas mixture, J. Comput. Phys. 18, 305-420 (1975)

11. Hass, B.L., Hash, D.B., Bird.G.A., Lumpkin III, F.E., Hassan, H.A.: Rates of thermal relaxation in direct simulation Monte Carlo methods, Phys. Fluids 6, 2191-2201 (1994)

12. Zhang, C., Schwartzentruber, T.E.: Inelastic collision selection procedures for direct simulation Monte Carlo calculations of gas mixtures, Phys. Fluids 25 (2013)

13. Lord, R.G.: Some extensions to the Cercignani–Lampis gas–surface scattering kernel. Phys. Fluids A: Fluid Dynamics 3, 706-710 (1991)

14. Sorensen, C., Valentini, P. and Schwartzentruber, T.E.: Uncertainty analysis of reaction rates in a finite-rate surface-catalysis model. J. Thermophys. 26(3), 407-416 (2012)

15. Scanlon, T.J., White, C., Borg, M.K., Palharini, R.C., Farbar, E., Boyd, I.D., Reese, J.M., Brown, R.E.: Open-source direct simulation Monte Carlo chemistry modeling for hypersonic flows. AIAA. J. 53(6), 1670-1680 (2015)

16. Boyd, I.D.: Modeling backward chemical rate processes in the direct simulation Monte Carlo method. Phys. Fluids 19(12) (2007)

17. Chapman, S., Cowling, T.G.: The mathematical theory of non-uniform gases, Cambridge (1970)

18. Jun, E., Gorji, M.H., Grabe, M., Hannemann, K.: Assessment of the cubic Fokker–Planck–DSMC hybrid method for hypersonic rarefied flows past a cylinder. Comput. Fluids 168, 1-13 (2018)

19. Jun, E., Boyd, I.D, Burt, J.M.: Assessment of an all-particle hybrid method for hypersonic rarefied flow. In 51st AIAA Aerospace Sciences Meeting including the New Horizons Forum and Aerospace Exposition (2013)

20. Wang, Z.H., Yu, Y.L. and Bao, L.: Heat transfer in nonequilibrium flows with homogeneous and heterogeneous recombination reactions. AIAA. J. 56(9), 3593-3599 (2018)